



# CHARACTERIZATION OF MULTIWALLED CARBON NANOTUBE-POLYMETHYL METHACRYLATE COMPOSITE RESINS AS DENTURE BASE MATERIALS

Russell Wang, DDS, MSD,<sup>a</sup> Junliang Tao, PhD,<sup>b</sup> Bill Yu, PhD,<sup>c</sup> and Liming Dai, PhD<sup>d</sup>

Case Western Reserve University School of Dental Medicine, and Case Western Reserve University School of Engineering, Cleveland, Ohio

**Statement of problem.** Most fractures of dentures occur during function, primarily because of the flexural fatigue of denture resins.

**Purpose.** The purpose of this study was to evaluate a polymethyl methacrylate denture base material modified with multiwalled carbon nanotubes in terms of fatigue resistance, flexural strength, and resilience.

**Material and methods.** Denture resin specimens were fabricated: control, 0.5 wt%, 1 wt%, and 2 wt% of multiwalled carbon nanotubes. Multiwalled carbon nanotubes were dispersed by sonication. Thermogravimetric analysis was used to determine quantitative dispersions of multiwalled carbon nanotubes in polymethyl methacrylate. Raman spectroscopic analyses were used to evaluate interfacial reactions between the multiwalled carbon nanotubes and the polymethyl methacrylate matrix. Groups with and without multiwalled carbon nanotubes were subjected to a 3-point-bending test for flexural strength. Resilience was derived from a stress and/or strain curve. Fatigue resistance was conducted by a 4-point bending test. Fractured surfaces were analyzed by scanning electron microscopy. One-way ANOVA and the Duncan tests were used to identify any statistical differences ( $\alpha=.05$ ).

**Results.** Thermogravimetric analysis verified the accurate amounts of multiwalled carbon nanotubes dispersed in the polymethyl methacrylate resin. Raman spectroscopy showed an interfacial reaction between the multiwalled carbon nanotubes and the polymethyl methacrylate matrix. Statistical analyses revealed significant differences in static and dynamic loadings among the groups. The worst mechanical properties were in the 2 wt% multiwalled carbon nanotubes ( $P<.05$ ), and 0.5 wt% and 1 wt% multiwalled carbon nanotubes significantly improved flexural strength and resilience. All multiwalled carbon nanotubes-polymethyl methacrylate groups showed poor fatigue resistance. The scanning electron microscopy results indicated more agglomerations in the 2% multiwalled carbon nanotubes.

**Conclusions.** Multiwalled carbon nanotubes-polymethyl methacrylate groups (0.5% and 1%) performed better than the control group during the static flexural test. The results indicated that 2 wt% multiwalled carbon nanotubes were not beneficial because of the inadequate dispersion of multiwalled carbon nanotubes in the polymethyl methacrylate matrix. Scanning electron microscopy analysis showed agglomerations on the fracture surface of 2 wt% multiwalled carbon nanotubes. The interfacial bonding between multiwalled carbon nanotubes and polymethyl methacrylate was weak based on the Raman data and dynamic loading results. (J Prosthet Dent 2014;111:318-326)

## CLINICAL IMPLICATIONS

Adding 0.5 wt% and 1 wt% of multiwalled carbon nanotubes improves the flexural strength and resilience of multiwalled carbon nanotubes-polymethyl methacrylate composite resins. Fatigue tests show that all groups with multiwalled carbon nanotubes had poor fatigue resistance. Future improvement of the material design and processing is needed.

<sup>a</sup>Associate Professor, Department of Comprehensive Care.

<sup>b</sup>Postgraduate student, Department of Civil Engineering.

<sup>c</sup>Associate Professor, Department of Civil Engineering.

<sup>d</sup>Professor, Department of Macromolecular Science and Engineering.

Most fractures of dentures occur during function, primarily from denture resin fatigue.<sup>1-4</sup> Flexural fatigue occurs after repeated flexing of a material; it is a mode of fracture whereby a structure eventually fails after being repeatedly subjected to small loads that individually are not detrimental to the component.<sup>5,6</sup> The midline fracture in dentures is often the result of flexural fatigue.<sup>5,7</sup> The reinforcement of denture base material has been a subject of interest to the dental material community. The fracture resistance of denture base polymers has been investigated.<sup>2,3,8-10</sup> Polymethyl methacrylate (PMMA) resin is the principal material of dental prostheses. To improve the properties of PMMA, a variety of materials have been incorporated into the polymer, including glass fibers, long carbon fibers, and metal wires.<sup>10-14</sup> Success has been limited.<sup>15,16</sup> The flexural strength of PMMA resin such as Lucitone199 (Dentsply Trubyte), which is a high-impact resin with butadiene and styrene additives, has been evaluated by several investigators and has yielded conflicting values but generally without significant material strengthening.<sup>17-19</sup>

Carbon nanotubes (CNT) have outstanding mechanical and electrical properties. CNTs have high mechanical properties with reported strengths 10 to 100 times higher than steel at a fraction of the weight.<sup>20-22</sup> CNTs are strong, resilient, and lightweight, and usually form stable cylindrical structures. CNTs that have a flawless structure are classified into 2 main types, namely single-walled and multiwalled CNTs (Fig. 1). Single-walled CNTs (SWCNT) consist of a single graphite sheet seamlessly wrapped into a cylindrical tube, and multiwalled CNTs (MWCNT) have an array of such nanotubes concentrically nested like the rings of a tree trunk. In addition to the exceptional mechanical properties associated with CNTs (elastic modulus of 1 TPa; diamond, 1.2 TPa), they also have superior thermal and electric properties.<sup>23,24</sup> To expand the potential applications of CNTs in polymer nanocomposites, an

understanding is needed of the properties of CNTs and the interfacial interactions between CNTs and the matrix. Although this requirement is no different from that for conventional fiber reinforced composites, the scale of the reinforcement phase diameter has changed from micrometers to nanometers.

The addition of carbon fibers to a matrix not only gives strength and elasticity to the material but also improves toughness.<sup>25</sup> Research on nanotube composites has focused on polymer-CNT based materials, wherein they exhibit mechanical properties that are superior to conventional polymer-based composites because of their considerably higher intrinsic strengths and moduli. The stress transfer efficiency can be 10 times higher than that of traditional additives.<sup>26</sup> MWCNTs seem to have a 'Russian nesting doll' structure, which has a set of patterns that consist of the same structure made in 2 halves. Inside it are a series of similar CNTs, each smaller than the last, placed one inside the other. Each constituent tubule is only bonded to its neighbors by weak Van der Waals forces. This may be an issue when adding CNTs to some polymer matrices without chemical bonding at CNTs-polymer interfaces.<sup>27</sup>

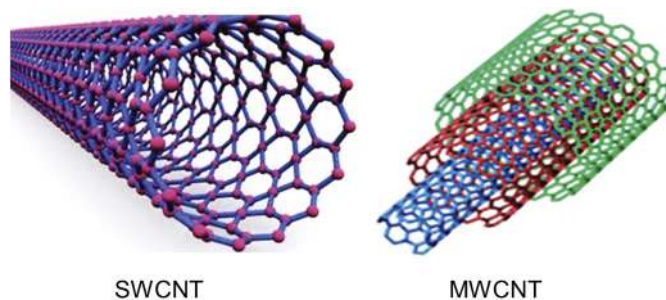
The second concern is the uniform dispersion of CNTs into a polymer matrix. Methods of using sonic dismembranators or chemical modification have been proposed.<sup>22,28,29</sup> The addition of CNTs usually causes a deformation mode of PMMA fibers. In pure PMMA fibers, polymer necking

occurs under increasing tension, which results in failure at relatively small strains. However, adding CNTs to a polymer may dramatically improve the resistance of the polymer to mechanical failure. Incorporating MWCNTs to polymer matrices may effectively bridge cracks and reduce the extent of plastic deformation by a PMMA matrix.<sup>30,31</sup> MWCNTs can successfully reinforce the fracture lines by strengthening the fibrils and bridging voids to enhance the fatigue performance of the polymer.

The effects of CNT reinforcement on the mechanical properties of denture base materials have not been explored. This investigation studied the effect of MWCNT reinforcement on the mechanical properties of a commonly used PMMA denture base material. The null hypothesis was that the addition of CNTs (MWCNTs by weight) would not improve the mechanical properties of the prosthesis.

## MATERIAL AND METHODS

Test specimens were fabricated with the denture base resin, Lucitone199 original shade (Dentsply Intl). The MWCNTs as received from the manufacturer (Designed Nanotubes LLC) were added to the measured acrylic monomer at 0.5% wt/wt, 1% wt/wt, and 2% wt/wt in a glass beaker. The liquid monomer was then ultrasonically mixed for 20 minutes (Model UP400S; Hielscher Ultrasonics GmbH). Manufacturer's instructions were followed with a powder-liquid ratio of



**1** Diagrammatic representation of single-walled nanotubes and multiwalled carbon nanotubes. Single-walled carbon nanotube: single graphite sheet seamlessly wrapped into cylindrical tube; multiwalled carbon nanotube: array of graphite sheets concentrically nested like rings of tree trunk.

21 g (32 mL):10 mL and a mixing time of 20 seconds with a vacuum mixer. Liquid monomer with and without MWCNTs was added to the powder and mixed for 20 seconds to ensure the wetting of all powder particles. The mix was covered for 9 minutes at room temperature and allowed to reach packing consistency. The mix was packed with conventional denture flasks (Hanau Type; Whip Mix Corp). Specimens were fabricated in a rectangular mold prepared in standard denture flasks by using a template that measured 70×40×3 mm. The closed flasks, tightened with spring clamps, were polymerized in a water bath for 9 hours at 71°C and cooled for 30 minutes in water at 26°C. The flask was bench cooled before deflasking. The specimens were removed from the flasks and cleaned of stone particles. After deflasking, each mold was cut to obtain the specimens of 70×10×3 mm for the flexural strength test. The specimens were sequentially polished with silicon carbide paper (1000, 800, and 600 grit) to achieve smooth edges.

The flexural strength was determined by using the 3-point bending test as specified by the International Organization for Standardization specification 20795-1:2008.<sup>32</sup> Four groups were prepared at 0%, 0.5%, 1%, and 2% of MWCNTs, with 7 specimens per group. The specimens were stored in distilled water at room temperature for 2 weeks before mechanical tests with a universal testing machine (Sintech Renew 1121; Instron Engineering Corp). Before each test, the specimen thickness and width were measured with a digital micrometer. A standard 3-point bending device was attached to the machine and connected to a computer. The testing parameter was set with a load of 4.448 kN and a crosshead speed of 0.5 mm/min.

The flexural strength (*S*) was calculated from the following formula:

$$S=3 FL/2 bd^2,$$

where: *S*, flexural strength in MPa; *F*, the load at break in N; *L*, 50 mm, the span of specimen between supports; *b*,

width of each specimen; and *d*, thickness of each specimen.

Based on the load-displacement (*F-Δ*) curves of the 3-point bending test, mechanical properties were determined. The load and displacement at the yield point was taken as the yield load (*F<sub>Y</sub>*) and the yield displacement (*Δ<sub>Y</sub>*). Stiffness was calculated based on 5% of the strain.

The moment of inertia about the bending axis (*I*) and the thickness (*t*) of each specimen was used to calculate resilience,  $\text{resilience}=0.5 (\text{yield stress} \times \text{yield strain})$ .<sup>33</sup> The fatigue test of the different groups was conducted with a Bionix II test system (MTS Inc). Pre-defined cyclic loading was applied to the 4-point supported beam until the beam was fractured. The cycle count to fracture was termed as the fatigue resistance.

The loading condition was controlled by the stroke of the tip of the actuator. First, after the beam was placed on the lower 2-point supports, the loading tip was lowered to contact the top surface of the beam. Once good initial contact was achieved, displacement of the loading tip was set at zero, and the center of the cyclic deflection was set as 3 mm; the loading function was then defined as a sine wave loading with a frequency of 5.7 Hz and a deflection of 2 mm. The applied forces and deflections of the loading tip were controlled by a computer. The number of the cycle count was recorded as fatigue resistance when the specimen was fractured, at which point the contact force began to show gross reduction. Seven MWCNTs-PMMA specimens of each group were tested. All specimens were stored in distilled water at room temperature for 2 weeks before testing.

Scanning electron microscopy (SEM) was performed on fractured specimens with a Hitachi scanning electron microscope (model S3200N). Images were acquired in the secondary electron mode with thermal field emission SEM. Raman spectroscopic analysis was conducted by using a visible laser light with the wavelength of 514 nm (Titan sapphire laser, Jobin-Yvon HR640

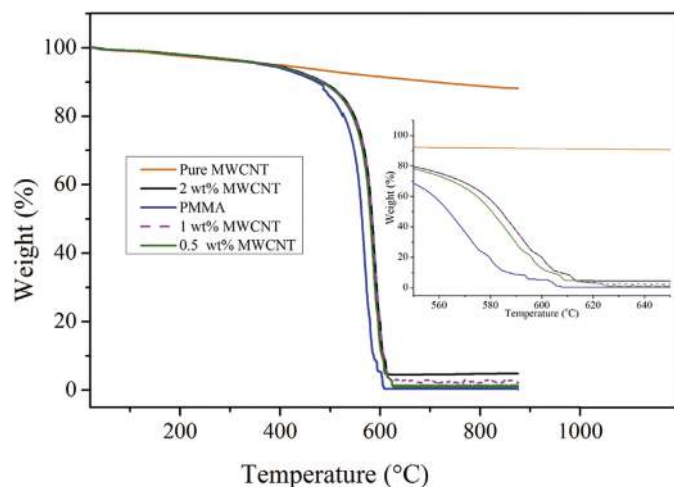
spectrometer) fitted with a charge-coupled device (CCD) detector. The laser with 50 mW was used to line and focus on each specimen throughout the procedure. Each specimen was tested at 3 different positions. Scattering data were acquired in a backscattering geometry. The thermal stability of each MWCNTs-PMMA composite resin specimens and confirmation of the amount of MWCNTs in PMMA were evaluated with thermogravimetric analysis (TGA). TGA measurements were performed with a thermogravimetric analyzer from 20°C to 800°C. The heating rate was 10°C/min with a nitrogen gas flow at 60 cm<sup>3</sup>/min rate.

Data derived from the control and the experimental groups on flexural strength, resilience, and fatigue resistance test were analyzed and compared by using 1-way ANOVA and the Duncan test to identify any statistical differences at ( $\alpha=.05$ ).

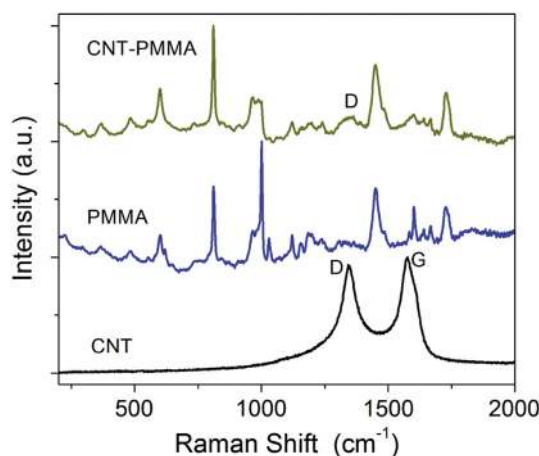
## RESULTS

The TGA curves of pure MWCNTs; pure Lucitone199 PMMA; and 0.5%, 1% and 2% MWCNTs-PMMA composite resin specimens are shown in Figure 2. Pure PMMA resin started to degrade in a nitrogen atmosphere at 300°C and was completely degraded at 600°C. For MWCNT-PMMA specimens, the percentage weight of MWCNTs was detected by TGA above 630°C after the PMMA was completely degraded, and the results accurately reflected the amount of MWCNTs for each specimen. The weights of the MWCNTs remain fairly constant at temperatures beyond 630°C (Fig. 1, insert).

The use of Raman spectroscopy in this study was to examine the purity of the MWCNTs and any interfacial reactions between the MWCNTs and the PMMA. Three arrays of the Raman spectra, which consist of pure MWCNTs, pure PMMA, and 2% MWCNTs in PMMA are shown in Figure 3. For the MWCNTs alone (Fig. 3, bottom of the 3 arrays), 2 unique peaks of graphitic structures were detected by Raman



**2** Thermogravimetric analysis curves of pure multiwalled carbon nanotubes. Pure Lucitone199 polymethyl methacrylate and 0.5%, 1%, and 2% multiwalled carbon nanotubes-polymethyl methacrylate composite resins.



**3** Raman spectra of pure multiwalled carbon nanotubes, pure polymethyl methacrylate, and 2% multiwalled carbon nanotubes in polymethyl methacrylate resin.

spectroscopy; one was located at  $1306\text{ cm}^{-1}$  designated to the D band ( $sp^3$  atomic orbital of carbon), and the second peak was located at  $1594\text{ cm}^{-1}$  designated to the G band ( $sp^2$  atomic orbital of carbon) associated with stretching motions of tangential C-C bonds. G band represents stable C-C bond inside MWCNTs and D band indicates defect graphitic structures or unstable C-C bonds. The array of the combined 2% MWCNTs and PMMA specimen show different intensities and locations of D and G band peaks, which confirms the interactions between MWCNTs and the PMMA matrix. Similar

patterns of Raman shifts of D and G bands of 0.5%, 1%, and 2% MWCNTs in PMMA are shown in Figure 4. The D band intensities decreased as the percentage of MWCNTs increased. The decreases in D band peaks in Figure 4 resulted from the interactions of unstable carbons with PMMA polymers. The peak ratios of D and G band changed from 0.93 for 0.5% MWCNTs to 0.84 for 2% MWCNTs. The results from the Raman spectroscopy analysis of the MWCNTs used in this study are identical to those of McNally et al.<sup>22</sup>

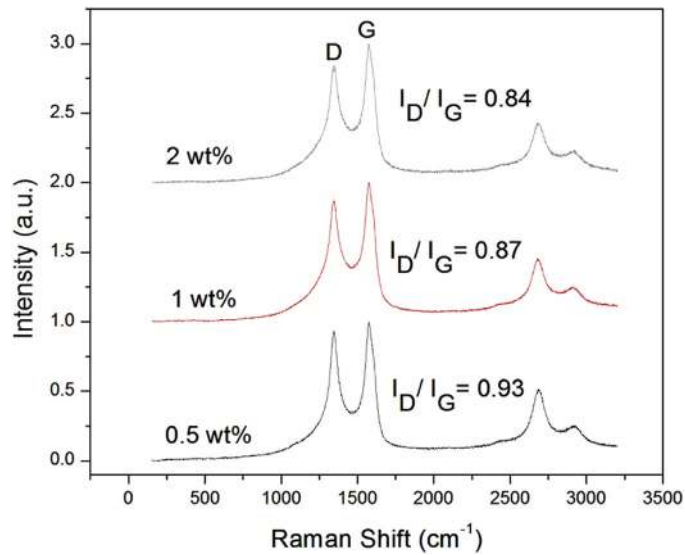
The results of the flexural strength test are shown in Figure 5. Compared

with the control group, flexural strength increased by an average of 9.3% with 0.5% and 3.9% with 1% MWCNTs-PMMA groups. However, an 11.4% decrease in flexural strength was noted for the 2% MWCNTs-PMMA group. The plot of resilience values for all groups is shown in Figure 6. There was an average 15.9% increase in resilience in the 0.5 wt% MWCNTs-PMMA group and 29% in the 1 wt% group. However, there was a 10.7% decrease in the 2 wt% MWCNTs-PMMA group when compared with the control group.

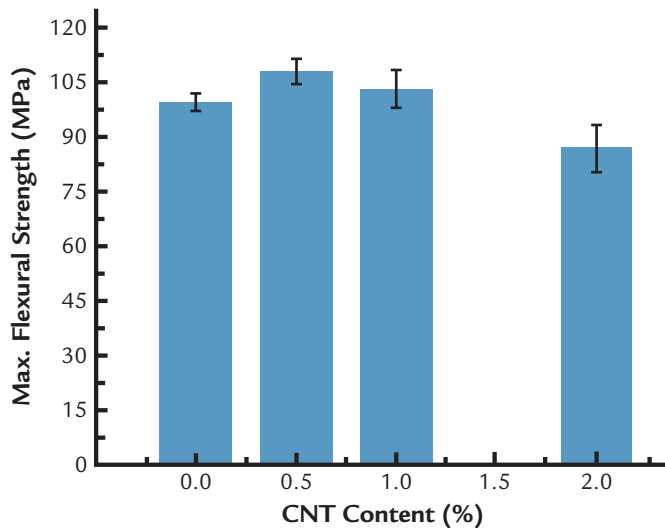
The equipment used for the 4-point bending fatigue test is shown in Figure 7A. A dynamic loading of fatigue resistance was determined by a typical loading curve, as shown in Figure 7B. When the beam was fractured, the contact forces between the beam and the loading tip were reduced and remained at a low level. The results of the fatigue resistance test for the 4 groups are shown in Figure 8. In contrast, fatigue resistance in all experimental groups decreased significantly (92.6% to 99.7%).

One-way ANOVA and the Duncan test showed statistical differences among the control and experimental groups (0.5%, 1%, and 2%) at a  $P$  value  $<.05$ . The level of MWCNTs significantly affected the PMMA's maximum flexural strength ( $P<.001$ ). When 0.5% of MWCNTs was used, maximum flexural strength ( $P<.001$ ) improved significantly compared with the control group. Resilience improved when MWCNTs were added to PMMA at the 0.5% and 1% level ( $P=.017$ ). When MWCNTs levels went from 1% to 2% ( $P=.008$ ), resilience weakened. A clear reverse effect of MWCNTs on the fatigue test ( $P<.001$ ) was observed as the wt% of MWCNTs increased.

The morphology and extent of dispersion of MWCNTs in the PMMA matrix was studied by SEM on fractured surfaces. The fractured surface at low magnification ( $\times 500$ ) if shown in Figure 9 and bundled MWCNTs and typical fractured surfaces of PMMA with 0.5% MWCNTs viewed perpendicular to the fractured surface



**4** Raman shifts of 0.5%, 1%, and 2% multiwalled carbon nanotubes-polymethyl methacrylate resins with different D-G band ratios.



**5** Flexural strength of polymethyl methacrylate with 0%, 0.5%, 1%, and 2% multiwalled carbon nanotubes.

( $\times 25\,000$ ) are shown in Figure 10. The MWCNTs can be clearly identified and are uniformly dispersed as single nanotubes. MWCNTs protrude from the fractured surface without PMMA coating. The center diameter of the MWCNTs and the concentric arrangement of the nanotubes are clearly evident. The overall diameter of the MWCNTs is approximately 25 to 35 nm. With 2% MWCNTs, more aggregates of varying dimensions are observed. In some instances, the PMMA seems to wrap around the MWCNTs (Fig. 11).

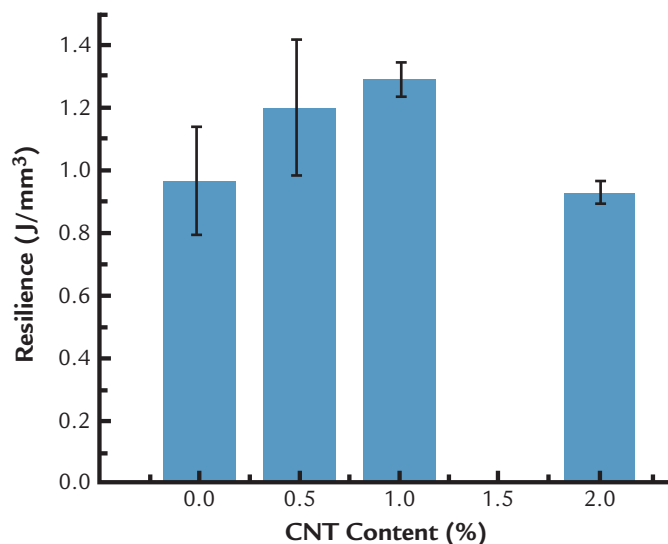
## DISCUSSION

This study was designed to investigate the potential applications of CNTs-PMMA composite resin as a dental base material. The hypothesis that the addition of MWCNTs would not improve the mechanical properties of the MWCNTs-PMMA composite resin was rejected based on the results of both static and dynamic loading tests. The purpose of using TGA in this study was to determine the dispersion of MWCNTs in the PMMA matrix quantitatively. The results confirm the

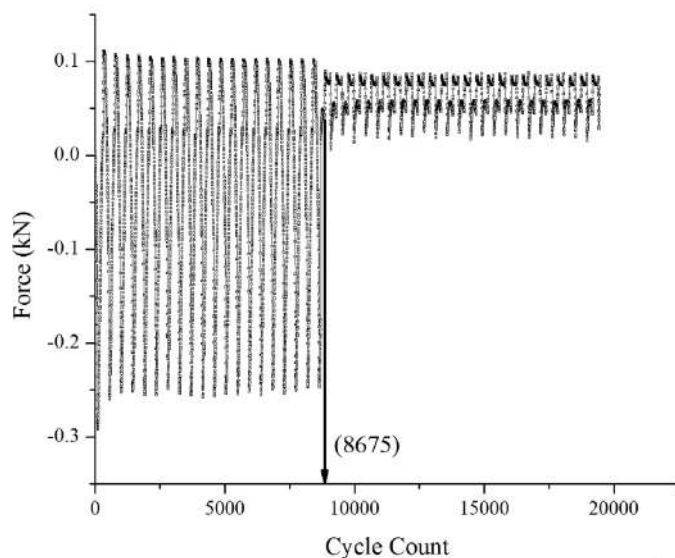
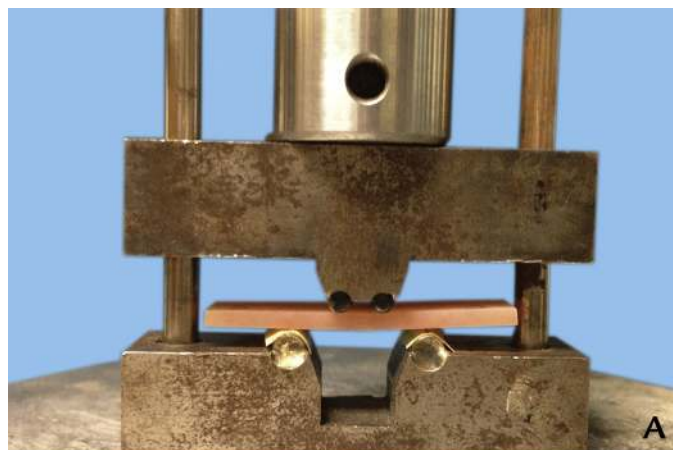
accurate amounts of MWCNTs in PMMA matrix for each group. The PMMA denture resin alone degrades from 380°C to 580°C based on the manufacturer's data. The data show that the PMMA was completely degraded at 600°C. As shown in Figure 2, the addition of MWCNTs in PMMA slightly improved the thermal stability of the PMMA resin because of the right shifts of TGA curves of 0.5%, 1%, and 2% MWCNTs-PMMA specimens higher than 500°C. However, TGA did not provide information on the qualitative distributions of MWCNTs in the PMMA matrix, namely, homogeneous or inhomogeneous dispersion of MWCNTs.

SEM was used to examine the qualitative analysis of MWCNTs dispersed in the PMMA matrix. Microscopic observations across the fractured surface indicated that the MWCNTs were well distributed and dispersed in the PMMA matrix when 0.5% and 1% were used. Once the MWCNTs reached 2% by weight, more agglomerations were noted. Microvoids on fractured surfaces also were detected by SEM. The MWCNTs-PMMA nanocomposite resin in this study was prepared by using high-power ultrasonic vibration. The results from SEM observations suggest that the preparation method in this study needs further improvement. The SEM results might explain the reason why the 2% MWCNTs-PMMA group had the lowest values in both static and dynamic loading tests. Results of studies have shown that MWCNTs tend to agglomerate when processed into polymers such as CNTs-polymer composite resins.<sup>22,29</sup> Individual nanotubes are difficult to separate during mixing. The current mixing method has limitations.

Another critical issue associated with the properties of the experimental MWCNTs-PMMA composite resins is the interfacial interaction-wetting between the polymer and the MWCNTs. Ideally, with good interfacial bonding between the PMMA and the MWCNTs, any load applied to the polymer matrix should be transferred to the nanotubes. In this study, Raman spectroscopy was



**6** Resilience values of polymethyl methacrylate resin with 0%, 0.5%, 1%, and 2% multiwalled carbon nanotubes.



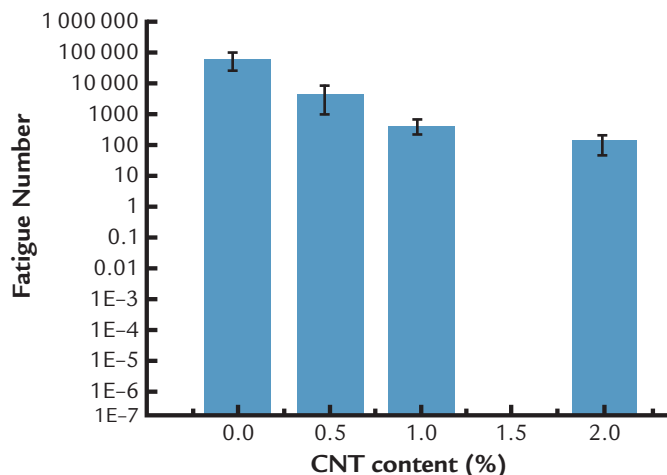
**7** A, Setup for 4-point bending fatigue test. B, Typical loading curve as function of loading vs cycle count for fatigue test.

used to examine the existence of interfacial bonding, and static and dynamic loading tests were used to qualify the interfacial bonding between MWCNTs and the PMMA matrix.

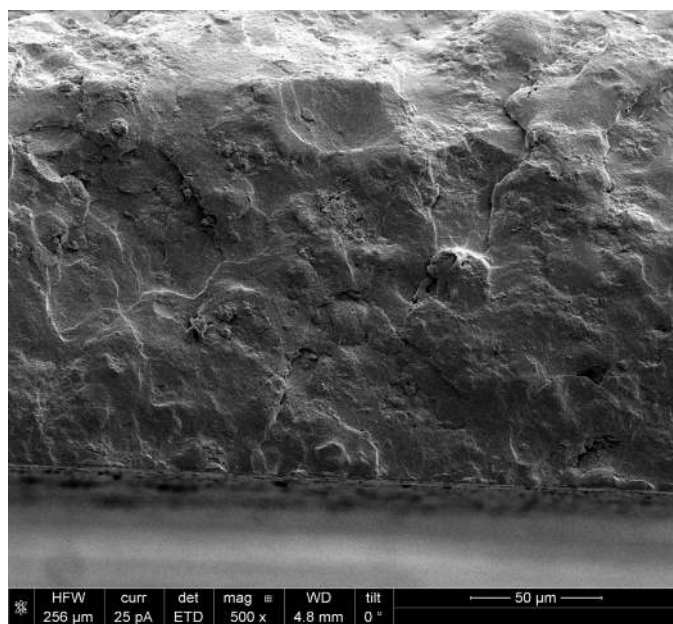
Raman spectroscopy is called the 'fingerprint' technique in that every chemical gives a unique Raman signal or spectrum and offers several advantages for microscopic analysis. Because it is a scattering technique, specimens do not need to be fixed or sectioned. Raman spectra can be collected from a small volume ( $<1 \mu\text{m}$  in diameter). Typically, in Raman spectroscopy, high-intensity laser radiation with wavelengths in either the visible or near-infrared regions of the spectrum is passed through a sample. Photons from the laser beam are absorbed by the molecules, exciting them to a higher energy state. If the molecules relax back to the vibrational state where they started, then the reemitted energy can be detected and recorded.

The spectrum of the Raman-scattered light depends on the molecular constituents present and their state, which allows the spectrum to be used for material identification and analysis. This can be used to gain information about the sample composition and structure determination in terms of chemical groups present and also its purity. The frequency differences between the excitation radiation and the Raman scattered radiation are called the Raman shift. Raman shifts are reported in units of wavenumber ( $\text{cm}^{-1}$ ) and are defined as  $\Delta (\text{cm}^{-1}) = (1/\lambda_o - 1/\lambda_R)$ , where  $\Delta$  is the Raman shift,  $\lambda_o$  is the laser wavelength, and  $\lambda_R$  is the Raman radiation wavelength. Each molecule has a unique characteristic array of light produced by the Raman effect, which can be plotted by intensity against the Raman shift on a Raman spectrum.

For CNTs, Raman spectroscopy can detect 2 unique peaks of graphitic structure: one is located at  $1306 \text{ cm}^{-1}$  designated to the D band ( $\text{sp}^3$  atomic orbital of carbon); the second peak is located at  $1594 \text{ cm}^{-1}$  designated to the G band ( $\text{sp}^2$  atomic orbital of carbon) associated with



**8** Fatigue resistance of polymethyl methacrylate resin with 0%, 0.5%, 1%, and 2% multiwalled carbon nanotubes.



**9** Low magnification scanning electron microscopy of typical fracture surface of multiwalled carbon nanotubes-polymethyl methacrylate composite. Scale bar=50 μm.

the stretching motions of tangential C-C bonds. A higher D band from CNTs indicates higher amorphous carbon atoms, which associate with crystallographic defects related to graphitic structures.

The observed shift in the Raman peaks of MWCNTs-PMMA in Figure 3 indicates the presence of interfacial interactions between MWCNTs and the polymer matrix. In Figure 4, the decrease of the ratios of the intensity of D- Raman peak and G- Raman peak (ID/IG) with the increase of MWCNTs content suggests that the polymer-nanotubes

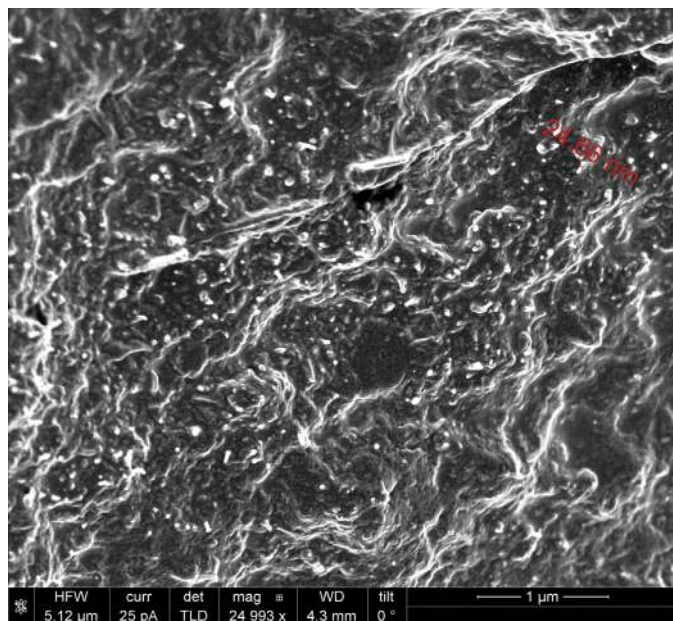
interactions had reduced the amorphous graphitic structures (D band) by interfacial reactions between MWCNTs and the PMMA matrix.

The Raman data in Figures 3 and 4 confirmed the interfacial reactions between MWCNTs and PMMA but did not give quantitative or qualitative information on interfacial bonding. Because some degree of interfacial bonding was present between MWCNTs and PMMA, 0.5% and 1% MWCNTs groups had better results than those of the control group for the static flexural strength test.

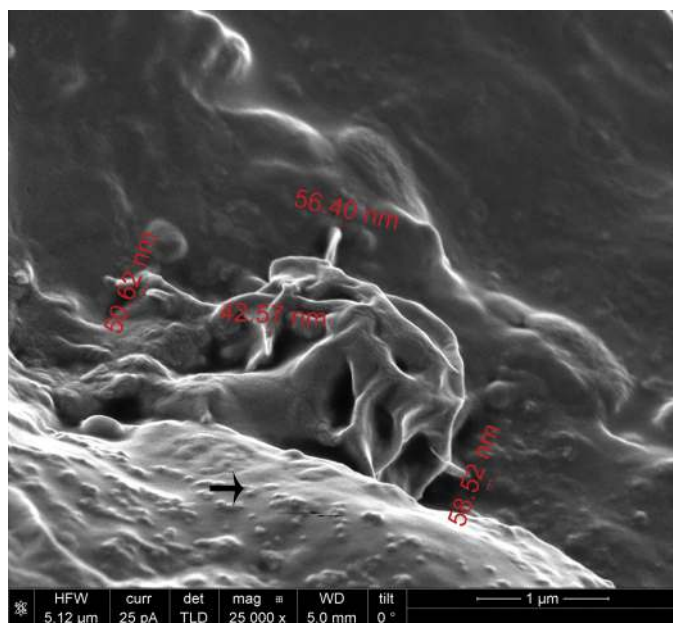
The 0.2% group had significantly lower values than the control group according to the static loading test, which likely resulted from the inhomogeneous dispersion of MWCNTs in the PMMA matrix. The negative effect of MWCNTs on PMMA resin, as shown by the dynamic fatigue test, was indicative of poor load transfer between polymer and MWCNTs. The crack propagation might intensify along numerous MWCNTs-PMMA interfacial locations.

Reported results on CNTs-polymer composite resin properties are scattered, depending on factors such as the types of CNTs (SWCNTs or MWCNTs), their morphology, diameter, length, and processing method. Other factors include the types of matrix and the interfacial interaction between CNTs and the matrix. Material design and processing are important steps in developing new denture based materials, followed by laboratory and clinical tests. Data from the study did not support the working hypothesis; this suggests that the system needs improvement. To address the material design issue, a future plan includes modifying the surface of MWCNTs to promote better interfacial interactions to polymers. Chemical, electrochemical, or plasma treatment could be useful to place different organ-functional groups on MWCNTs. Adding carboxyl or amide functional groups to MWCNTs would be a logical approach to facilitate MWCNTs-PMMA interfacial reactions. Another approach would be to use an oxidation or silanization process to modify the surface of CNTs with a low-pressure oxygen plasma treatment. For material processing of MWCNTs to PMMA, the future addition of surfactants to PMMA monomer-MWCNTs during mixing may provide a better solution to the homogenous dispersion of MWCNTs to a polymer material.

The color of CNTs can be determined by the amounts of conjugated double bonds of carbons. Various color modifications of MWCNTs can be done by attaching other functional groups, which would change the color of CNTs. This is beyond the scope of



**10** Bundled multiwalled carbon nanotubes and typical fracture surface of polymethyl methacrylate resin with 0.5% multiwalled carbon nanotubes. Scale bar=1  $\mu$ m.



**11** Micrograph of fracture surface of 2% multiwalled carbon nanotubes-polymethyl methacrylatespecimen. Center of the image shows agglomeration multiwalled carbon nanotubes and arrows are single fibrils multiwalled carbon nanotubes. Scale bar=1  $\mu$ m.

this article and would be important for a future study. Other alternatives are to use SWCNTs, which are transparent or use fewer MWCNTs in the PMMA matrix.

Further study is needed to improve the dispersion of MWCNTs into commercial denture base systems and

thereby allows the effects of MWCNTs on the denture base materials to be tested as they are prepared in clinical situations. Future investigations will also center on enhancing the bonding of MWCNTs to the PMMA denture base material to reduce denture failures.

## CONCLUSIONS

TGA showed accurate quantitative dispersions of MWCNTs in the PMMA matrix. Raman spectroscopy showed that an interfacial reaction occurred between MWCNTs and the PMMA matrix. The results from the static and dynamic loading test suggested that the interfacial bonding between MWCNTs and PMMA was weak and in need of improvement. The addition of 0.5% and 1% MWCNTs improved the PMMA resin flexural strength and resilience but not the 2% MWCNTs because of poor dispersion of MWCNTs based on SEM observations. MWCNT adversely affected the fatigue resistance of MWCNT-PMMA composite resins, with fatigue resistance deteriorating with higher concentrations of MWCNTs.

## REFERENCES

1. Gurbuz O, Unalan F, Dikbas I. Comparative study of the fatigue strength of five acrylic denture resins. *J Mech Behav Biomed Mater* 2010;3:636-9.
2. Machado C, Sanchez E, Azer SS, Uribe JM. Comparative study of the transverse strength of three denture base materials. *J Dent* 2005;35:930-3.
3. Smith LT, Powers JM, Ladd D. Mechanical properties of new denture resins polymerized by visible light, heat, and microwave energy. *Int J Prosthodont* 1992;5:315-20.
4. Stafford GD, Lewis TT, Huggett R. Fatigue of testing of denture base polymers. *J Oral Rehabil* 1982;9:139-54.
5. Diaz-Arnold AM, Vargas MA, Shaull K, Laffoon JE, Qian F. Flexural and fatigue strengths of denture base resin. *J Prosthet Dent* 2008;100:47-51.
6. Fujii K. Fatigue properties of acrylic denture base resins. *Dent Mater J* 1989;8:243-59.
7. Darbar UR, Huggett R, Harrison A. Denture fracture: a survey. *Br Dent J* 1994;176:342-5.
8. Vuorine AM, Dyer SR, Lassila LV, Vallittu PK. Effect of rigid rod polymer filler on mechanical properties of poly-methyl methacrylate denture base material. *Dent Mater* 2008;24:708-13.
9. Kim SH, Watts DC. The effect of reinforcement with woven E-glass fibers on the impact strength of complete dentures fabricated with high-impact acrylic resin. *J Prosthet Dent* 2004;91:274-80.
10. Jagger DC, Jagger RG, Allen SM, Harrison A. An investigation into the transverse and impact strength of 'high strength' denture base resins. *J Oral Rehabil* 2002;29:263-7.
11. Franklin P, Wood DJ, Bubbs NL. Reinforcement of poly (methyl methacrylate) denture base with glass flake. *Dent Mater* 2005;24:365-70.



12. Kuehn KD, Ege W, Gopp U. Acrylic bone cements: composition and properties. *J Orthop Clin North Am* 2005;36:17-28.
13. Stipho HD. Effect of glass fiber reinforcement on some mechanical properties of autopolymerizing polymethyl methacrylate. *J Prosthet Dent* 1998;79:580-4.
14. Bowman AJ, Manley TR. The elimination of breakages in upper dentures by reinforcement with carbon fibers. *Br Dent J* 1984;156:87-9.
15. Zappini G, Kammann A, Wachter W. Comparison of fracture tests of denture base materials. *J Prosthet Dent* 2003;90:578-85.
16. Narva KK, Lassila LV, Vallittu PK. The static strength and modulus of fiber reinforced denture base polymer. *Dent Mater* 2005;21:421-8.
17. Chai J, Takahashi Y, Kawaguchi M. The flexural strengths of denture base acrylic resins after relining with a visible-light-activated material. *Int J Prosthet Dent* 1998;11:121-4.
18. Dixon DL, Fincher M, Breeding LC, Mueninghoff LA. Mechanical properties of a light polymerizing provisional restorative material with and without reinforcement fibers. *J Prosthet Dent* 1995;73:510-4.
19. Khan Z, Von Fraunhofer JA, Razavi R. The staining characteristics, transverse strength and microhardness of a visible light cured denture base material. *J Prosthet Dent* 1987;57:384-7.
20. Thostenson ER, Chou T. Advances in the science and technology of carbon nanotubes and their composites: a review. *Comp Sci Technol* 2004;61:1899-912.
21. Ci L, Suhr J, Pushparaj V, Zhang X, Ajayan PM. Continuous carbon nanotubes reinforced composites. *Nano Lett* 2008;9:2762-6.
22. McNally T, Potschke P, Halley P, Murphy M, Martin D, Bell S, et al. Polyethylene multiwalled carbon nanotube composites. *Polymer* 2005;46:8222-32.
23. Fiedler B, Gojny F, Wichmann MH, Nolte MC, Schulte K. Fundamental aspects of nano-reinforced composites. *Compos Sci Technol* 2006;16:3115-25.
24. Cadek M, Coleman NJ, Barron J, Hedicke K, Blau WJ. Morphological and mechanical properties of carbon-nanotubes-reinforced semicrystalline and amorphous polymer composites. *Appl Phys Lett* 2002;81:5123-8.
25. Harris P. Carbon nanotubes and related structures. Cambridge: Cambridge University Press; 2002. p. 202.
26. Iijima S. Helical microtubules of graphitic carbon. *Nature* 1991;354:56-8.
27. Baughman RH, Zakhidov AA, de Heer WA. Carbon nanotubes: the route toward applications. *Science* 2002;297:787-92.
28. Safadi B, Grulke EA. Multiwalled carbon nanotube polymer composites: synthesis and characterization of thin films. *J App Polymer Sci* 2002;84:2260-9.
29. Marrs B, Andrews R, Rantell T, Pienkowski D. Augmentation of acrylic bone cement with multiwall carbon nanotubes. *J Biomed Mater Res A* 2006;77:269-76.
30. Sui X, Wagner HD. Tough nanocomposites: the role of carbon nanotubes type. *Nano Lett* 2009;9:1423-36.
31. Ormsby R, McNally T, Mitchell C, Dunne N. Influence of multiwall carbon nanotubes functionality and loading on mechanical properties of PMMA/MWCNT bone cements. *J Mater Sci Med* 2010;21:2287-92.
32. International Organization for Standardization, ISO 20795-1:2008, Dentistry—BasePolymers—Part 1: Denture Base Polymers. Geneva: ISO.
33. Akkus O, Adar F, Schaffler MB. Age-related changes in physicochemical properties of mineral crystals are related to impaired mechanical function of cortical bone. *Bone* 2004;34:443-53.

Corresponding author:

Dr Russell Wang  
 Department of Comprehensive Care  
 Case Western Reserve University School of  
 Dental Medicine  
 10900 Euclid Ave  
 Cleveland, OH 44106-4905  
 E-mail: rxw26@case.edu

Copyright © 2014 by the Editorial Council for  
*The Journal of Prosthetic Dentistry.*

### Availability of Journal Back Issues

As a service to our subscribers, copies of back issues of *The Journal of Prosthetic Dentistry* for the preceding 5 years are maintained and are available for purchase from Elsevier, Inc until inventory is depleted. Please write to Elsevier, Inc, Subscription Customer Service, 6277 Sea Harbor Dr, Orlando, FL 32887, or call 800-654-2452 or 407-345-4000 for information on availability of particular issues and prices.